Comptes Rendus

Mathématique

Kamran, Amjad Ali and José Francisco Gómez-Aguilar

A transform based local RBF method for 2D linear PDE with Caputo–Fabrizio derivative

Numerical Analysis / *Analyse numérique*

A transform based local RBF method for 2D linear PDE with Caputo–Fabrizio derivative

Kamran [*, a]**, Amjad Ali** [b] **and José Francisco Gómez-Aguilar** [c]

[a] Department of Mathematics, Islamia College Peshawar, Khyber Pakhtoon Khwa, Pakistan.

[b] Department of Basic Sciences and Islamiat, University of Engineering and Technology Peshawar,Khyber Pakhtoon Khwa, Pakistan.

[c] CONACyT-Tecnológico Nacional de México/CENIDET.Interior Internado Palmira S/N, Col. Palmira, C.P.62490, Cuernavaca, Morelos, México.

E-mails: kamran.maths@uetpeshawar.edu.pk, amjad_puet@yahoo.com, jgomez@cenidet.edu.mx

Abstract. The present work aims to approximate the solution of linear time fractional PDE with Caputo Fabrizio derivative. For the said purpose Laplace transform with local radial basis functions is used. The Laplace transform is applied to obtain the corresponding time independent equation in Laplace space and then the local RBFs are employed for spatial discretization. The solution is then represented as a contour integral in the complex space, which is approximated by trapezoidal rule with high accuracy. The application of Laplace transform avoids the time stepping procedure which commonly encounters the time instability issues. The convergence of the method is discussed also we have derived the bounds for the stability constant of the differentiation matrix of our proposed numerical scheme. The efficiency of the method is demonstrated with the help of numerical examples. For our numerical experiments we have selected three different domains, in the first test case the square domain is selected, for the second test the circular domain is considered, while for third case the L-shape domain is selected.

1. Introduction

Fractional calculus is the branch of mathematics in which the differential or integral operators with arbitrary orders are studied. Fractional calculus offers new features in describing complex dynamics of realistic systems having memory effect. Fractional order differential equations can

---

be used to model various processes related to complicated system of several areas of engineering and sciences. In literature a lot of valuable work is available in which the authors have studied various fractional derivatives and their applications. The investigation of numerous phenomena like electrodynamics, elasticity, diffusion process, fluid flow, signal and image processing, hydrology and many others can be done with the help of fractional PDEs [4, 17]. In [22] Samko et al. studied various types of fractional derivatives such as Grünwald–Letnikov, Caputo, Marchaud, Riemann–Liouville and many more. More work on fractional derivatives and their applications can be found in [7, 13, 14, 18, 21, 24] and the references therein. However these classical fractional derivatives have a singular kernel, and hence they may face difficulties in describing the non locality of real world dynamics.

In order to handle the non local systems in a better way, recently a new fractional derivative is introduced in [6] called Caputo–Fabrizio(CF) fractional derivative which has attracted the attention of researchers and has become much popular among the researchers. Because of the smooth kernel the CF derivative has numerous applications. The CF derivative has been successfully applied to model groundwater flowing within a confine and unconfined aquifer [4, 10], ground water pollution [5], salute transport and non Darcian flow [25], mass-spring damper system [11], HIV model [2], Mathematical biological model [12] and their references.

The researchers have developed various methods for modeling the numerical and the analytical solutions of time-fractional order PDEs with CF derivative. In [17] the authors have solved linear PDEs with CF derivative using Laplace homotopy analysis method. The model of groundwater flow within confined aquifer with CF derivative [4] is solved using Sumudu transform. In [3] CF derivative is applied to Fisher's diffusion equation and the solution is presented using some iterative method. The Allen Cahn model with CF derivative is solved using Crank–Nicholson scheme [1]. In [5] the author's studied numerical approximation of space-time CF fractional derivative and its application to groundwater pollution equation via Crank–Nicholson scheme. In [16] the authors have obtained the fundamental solution of advection-diffusion problem with CF derivative using Laplace and Fourier transforms. The authors in [9] have analyzed the rock fracture process mathematically and applied the CF derivative. Other analytical or numerical methods that could be of interest are given in [8, 19, 20] and the references therein.

In this article we propose a numerical scheme which is based on the Laplace transform(LT) and local radial basis functions (RBFs) for the approximation of the solution of linear time fractional PDEs with CF derivative over complex domians. The purpose of combining the Laplace transformation and local (RBFs) is to avoid the time stepping procedure. The advantage of using the Laplace transformation is the less computational cost and no time instability issue.

2. Basic definitions from fractional calculus:

Definition 1. *The Laplace transform of a function $g(t)$ is denoted by $\mathcal{L}[g(t)] = \widehat{g}(s)$, and is defined as*

$$\mathcal{L}[g(t)] = \widehat{g}(s) = \int_0^\infty e^{st} g(t) dt. \tag{1}$$

Definition 2. *The Caputo–Fabrizio (CF) fractional derivative is defined as [3, 17]*

$$\substack{CF \\ 0}D_t^\alpha g(t) = \frac{(2-\alpha)M(\alpha)}{2(1-\alpha)} \int_0^t exp\left(\frac{-\alpha}{1-\alpha}(t-s)\right) g^{(n)}(s) ds, \ \alpha \in (n-1, n), \tag{2}$$

where $M \in \mathbb{R}$ satisfying the condition $M(0) = M(1) = 1$.

Definition 3. *If $\alpha \in (0,1)$ and $n \in \mathbb{N}$, then the Laplace transform of the CF derivative is defined as [3, 17]*

$$\mathcal{L}\left[\substack{CF \\ 0}D_t^{\alpha+n} g(t)\right](s) = \frac{s^{n+1}\widehat{g}(s) - s^n g(0) - s^{n-1}g^{(1)}(0) - \ldots - g^{(n)}(0)}{s + \alpha(1-s)}. \tag{3}$$

using n = 0 we get

$$\mathscr{L}\left[{}^{CF}_0 D_t^\alpha g(t)\right](s) = \frac{s\widehat{g}(s) - g(0)}{s + \alpha(1-s)}, \tag{4}$$

similarly for n = 1 we get

$$\mathscr{L}\left[{}^{CF}_0 D_t^{\alpha+1} g(t)\right](s) = \frac{s^2\widehat{g}(s) - sg(0) - g^{(1)}(0)}{s + \alpha(1-s)}. \tag{5}$$

3. Proposed Scheme

To derive our proposed numerical scheme we consider a linear PDE with Caputo–Fabrizio derivative ($m-1 < \alpha + n \le m$):

$$ {}^{CF}_0 D_t^\alpha g(\mathbf{x}, t) - \mathscr{L} g(\mathbf{x}, t) = \rho(\mathbf{x}, t), \quad \text{where} \quad \mathbf{x} \in \Omega, \quad \text{and} \quad t \in [0, T], \tag{6}$$

with initial and boundary conditions are

$$\partial_t^k g(\mathbf{x}, 0) = g_k(\mathbf{x}), k = 0, 1, \dots, m-1, \mathbf{x} \in \Omega,$$

and

$$\mathscr{B} g(\mathbf{x}, t) = \epsilon(\mathbf{x}, t), \mathbf{x} \in \partial\Omega. \tag{7}$$

The application of Laplace transformation to (6) and (7) gives the following equations

$$\mathscr{L}\left[{}^{CF}_0 D_\tau^{\alpha+n} g(\mathbf{x}, t) - \mathscr{L} g(\mathbf{x}, t)\right] = \mathscr{L}\left[\rho(\mathbf{x}, t)\right] \tag{8}$$

and

$$\mathscr{B} \widehat{g}(\mathbf{x}, s) = \epsilon_1(\mathbf{x}, s). \tag{9}$$

From Equation (8) we have,

$$\frac{s^{n+1}\widehat{g}(\mathbf{x}, s) - s^n g(\mathbf{x}, 0) - s^{n-1} g^{(1)}(\mathbf{x}, 0) - \dots - g^{(n)}(\mathbf{x}, 0)}{s + \alpha(1-s)} - \mathscr{L}\widehat{g}(\mathbf{x}, s) = \widehat{\rho}(\mathbf{x}, s) \tag{10}$$

thus we get the following system,

$$\left[\left(\frac{s^{n+1}}{s + \alpha(1-s)}\right) I - \mathscr{L}\right] \widehat{g}(\mathbf{x}, s) = \widehat{h}(\mathbf{x}, s), \mathbf{x} \in \Omega, \tag{11}$$

$$\mathscr{B} \widehat{g}(\mathbf{x}, s) = \epsilon_1(\mathbf{x}, s), \mathbf{x} \in \partial\Omega, \tag{12}$$

where I is the identity operator and the value of $\widehat{h}(\mathbf{x}, s)$ is

$$\widehat{h}(\mathbf{x}, s) = \frac{s^n g(\mathbf{x}, 0) + s^{n-1} g^{(1)}(\mathbf{x}, 0) + \dots + g^{(n)}(\mathbf{x}, 0)}{s + \alpha(1-s)} + \widehat{\rho}(\mathbf{x}, s).$$

In our method first we represent the solution $g(\mathbf{x}, t)$ of the original problem (6)-(7) as a contour integral

$$g(\mathbf{x}, t) = \frac{1}{2\pi i} \int_\Gamma e^{st} \widehat{g}(\mathbf{x}, s) \, ds, \tag{13}$$

where, for $Res \ge \omega$ with ω appropriately large, and Γ is an initially appropriately chosen line Γ_0 perpendicular to the real axis in the complex plane, with $Ims \to \pm\infty$. The integral (13) is just the inverse transform of $\widehat{g}(\mathbf{x}, t)$, with the condition that it must be analytic to the right of Γ_0. To make sure the contour of integration remains in the domain of analyticity of $\widehat{g}(\mathbf{x}, t)$, we select Γ as a deformed contour in the set $\Sigma_\phi^\omega = \{s \ne 0 : |args| < \phi\} \cup \{0\}$, which behaves as a pair of asymptotes in the left half plane, with $Res \to -\infty$ when $Ims \to \pm\infty$, which force e^{st} to decay towards both ends of Γ. In our work we choose Γ as

$$s(\xi) = \omega + \lambda(1 - \sin(\delta - \iota\xi)), \xi \in \mathbb{R}, \,(\Gamma) \tag{14}$$

where,

$$\lambda > 0,\ 0 < \delta < \phi - \frac{\pi}{2}, \quad \text{and} \quad \omega > 0. \tag{15}$$

By writing $s = x + \iota y$, we notice that (14) is the left branch of the following hyperbola

$$\left(\frac{x - \omega - \lambda}{\lambda \sin\delta}\right)^2 - \left(\frac{y}{\lambda \cos\delta}\right)^2 = 1, \tag{16}$$

the asymptotes for (16) are $y = \pm(x - \omega - \lambda)\cot\delta$, and x-intercept at $s = \omega + \lambda(1 - \sin\delta)$. The condition (15) confirms that Γ lies in the sector $\Sigma^\omega_\phi = \omega + \Sigma_\phi \subset \Sigma_\phi$, and grows into the left half plane. From (14) and (13), we get

$$g(\mathbf{x}, t) = \frac{1}{2\pi i} \int_{-\infty}^{\infty} e^{s(\xi)t} \widehat{g}(\mathbf{x}, s(\xi)) \acute{s}(\xi) d\xi. \tag{17}$$

The trapezoidal rule is used for the approximation of Equation (17) with step k as follows

$$g_k(\mathbf{x}, t) = \frac{k}{2\pi i} \sum_{j=-M}^{M} e^{s_j t} \widehat{g}\left(\mathbf{x}, s_j\right) \acute{s}_j,\ \xi_j = jk,\ s_j = s\left(\xi_j\right),\ s'_j = s'\left(\xi_j\right). \tag{18}$$

To obtain the solution $g_k(\mathbf{x}, t)$, first we must solve system of $2M+1$ equations given in (11)-(12) for quadrature points s_j, $|j| \le M$. For this purpose the local RBF method is used to discretize the operators $\mathcal{L}$, and $\mathcal{B}$.

3.1. *Local RBF approximation*

Given a set of points $\{\mathbf{x}_i\}_{i=1}^N$ in $\mathbb{R}^d$, where $d \ge 1$ the approximate function for $\widehat{g}(\mathbf{x})$ using local RBF method has the form,

$$\widehat{g}(\mathbf{x}_i) = \sum_{\mathbf{x}_j \in \Omega_i} \lambda_j^i \phi\left(\left\|\mathbf{x}_i - \mathbf{x}_j^i\right\|\right), \tag{19}$$

where $\boldsymbol{\lambda}^i = \{\lambda_j^i\}_{j=1}^n$ is the expansion coefficients vector, $\phi(r)$ is a kernel function, the distance between $\mathbf{x}_i$ and $\mathbf{x}_j$ is $r = \|\mathbf{x}_i - \mathbf{x}_j\|$. Ω, and Ω_i are global domain and local domains respectively. The sub-domain Ω_i contains the center $\mathbf{x}_i$, and around it, its n neighboring centers. Thus we obtain $n \times n$ linear systems

$$\begin{pmatrix} \widehat{g}\left(\mathbf{x}_1^i\right) \\ \widehat{g}\left(\mathbf{x}_2^i\right) \\ . \\ . \\ . \\ \widehat{g}(\mathbf{x}_n^i) \end{pmatrix} = \begin{pmatrix} \phi\left(\left\|\mathbf{x}_1^i - \mathbf{x}_1^i\right\|\right) & \phi\left(\left\|\mathbf{x}_1^i - \mathbf{x}_2^i\right\|\right) & \dots & \phi\left(\left\|\mathbf{x}_1^i - \mathbf{x}_n^i\right\|\right) \\ \phi\left(\left\|\mathbf{x}_2^i - \mathbf{x}_1^i\right\|\right) & \phi\left(\left\|\mathbf{x}_2^i - \mathbf{x}_2^i\right\|\right) & \dots & \phi\left(\left\|\mathbf{x}_2^i - \mathbf{x}_n^i\right\|\right) \\ . & . & . & . \\ . & . & . & . \\ . & . & . & . \\ \phi\left(\left\|\mathbf{x}_n^i - \mathbf{x}_1^i\right\|\right) & \phi\left(\left\|\mathbf{x}_n^i - \mathbf{x}_2^i\right\|\right) & \dots & \phi\left(\left\|\mathbf{x}_n^i - \mathbf{x}_n^i\right\|\right) \end{pmatrix} \begin{pmatrix} \lambda_1^i \\ \lambda_2^i \\ . \\ . \\ . \\ \lambda_n^i \end{pmatrix},\ i = 1, 2, \dots, N, \tag{20}$$

which can be written as,

$$\widehat{\boldsymbol{g}}^i = \Phi^i \boldsymbol{\lambda}^i,\ 1 \le\ i\ \le N, \tag{21}$$

the matrix Φ^i contains elements in the form $b_{kj}^i = \phi(\|\mathbf{x}_k^i - \mathbf{x}_j^i\|)$, where $\mathbf{x}_k^i, \mathbf{x}_j^i \in \Omega_i$, the unknowns $\boldsymbol{\lambda}^i = \{\lambda_j^i : j = 1, \dots, n\}$ are obtained by solving each of the N systems in (21). For the differential operator $\mathcal{L}$ we have the form,

$$\mathcal{L}\widehat{g}(\mathbf{x}_i) = \sum_{\mathbf{x}_j \in \Omega_i} \boldsymbol{\lambda}_j^i \mathcal{L}\phi\left(\left\|\mathbf{x}_i - \mathbf{x}_j^i\right\|\right), \tag{22}$$

the above Equation (22) can be expressed as a dot product

$$\mathcal{L}\widehat{g}(\mathbf{x}_i) = \boldsymbol{\lambda}^i \cdot \boldsymbol{v}^i, \tag{23}$$

where $\boldsymbol{v}^i$ is a n-row vector and $\boldsymbol{\lambda}^i$ is a n-column vector, entries of the n-column vector $\boldsymbol{v}^i$ are given as

$$\boldsymbol{v}^i = \mathcal{L}\phi\left(\left\|\mathbf{x}_i - \mathbf{x}_j^i\right\|\right),\ \mathbf{x}_j^i \in \Omega_i, \tag{24}$$

eliminating the co efficient $\boldsymbol{\lambda}^i$ from (21), and (23) we have the following expression

$$\mathscr{L}\widehat{g}(\boldsymbol{\chi}_i) = \boldsymbol{v}^i\left(\Phi^i\right)^{-1}\widehat{\boldsymbol{g}}^i = \varpi^i\widehat{\boldsymbol{g}}^i \tag{25}$$

where,

$$\varpi^i = \boldsymbol{v}^i\left(\Phi^i\right)^{-1}, \tag{26}$$

thus at each node $\mathbf{x}_i$ the approximation of the operator $\mathscr{L}$ via local meshless method is given as

$$\mathscr{L}\widehat{g} \equiv \mathbf{D}\widehat{\boldsymbol{g}}, \tag{27}$$

In Equation (27), D is a sparse differentiation matrix obtained via localized RBF method as an approximation to $\mathscr{L}$. The matrix D has order $N \times N$, it has n non-zero elements, and $N - n$ zero elements, where N is number of centers in global domain, and n is the number of centers local domain. The boundary operator $\mathscr{B}$ can be discretized in similar way.

4. Convergence and Accuracy

For the approximation of linear differential equations with CF derivative using our proposed method, the localized RBF method and Laplace transformation is used. In our numerical scheme the time variable is eliminated using Laplace transform, and this process causes no error. Then the localized RBF method is utilized for approximating time independent equation. The error estimate for localized RBF method is of order $O(\eta^{\frac{1}{\epsilon h}}), 0 < \eta < 1$, ϵ is the shape parameter and h is the fill distance. In the process of approximating the integral (17) convergence is achieved at different rates depending on the path Γ. In approximating the integral (17) the convergence order rely upon on the step k of the quadrature rule and the time domain $[t_0, T]$. The proof for the order of quadrature error is given in the next Theorem 4.

Theorem 4 ([15, Theorem 2.1]). *Let $g(\mathbf{x}, t)$ be the solution of (6)-(7) with $\widehat{g}(\mathbf{x}, t)$ analytic in Σ_ϕ^ω. Let $\Gamma \subset \Omega_r \subset \Sigma_\phi^\omega$, and define $b > 0$ by*

$$cosh b = \frac{1}{\theta\tau\sin(\delta)} \quad where \quad \tau = \frac{t_0}{T}, \quad 0 < t_0 < T, 0 < \theta < 1.0 \quad and \ let \ \lambda = \frac{\theta\overline{r}M}{bT}.$$

Then for equation (19), with $k = \frac{b}{M} \le \frac{\overline{r}}{log2}$, we have

$$\left|g(\mathbf{x}, t) - g_k(\mathbf{x}, t)\right| \le CQe^{\omega\tau} l\left(\rho_r M\right) e^{-\mu M}\left(\|g_0\| + \left\|\widehat{\rho}(\mathbf{x}, t)\right\|_{\Sigma_\phi^\omega}\right),$$

for $\mu = \frac{\overline{r}(1-\theta)}{b}$, $d\rho_r = \frac{\theta\overline{r}\tau\sin(\delta - r_1)}{b}$, $\overline{r} = 2\pi r_1$, $r_1 > 0$, $t_0 \le \tau \le T$, $C = C_{\delta, r_1, \beta}$ and

$$l(x) = \max\left(1, log\left(\frac{1}{x}\right)\right).$$

Hence the error estimate for the proposed scheme is

$$error_{est} = \left|g_k(\mathbf{x}, t) - g(\mathbf{x}, t)\right| = O\left(e^{-\mu M}\right) l\left(\rho_r M\right).$$

5. Stability

To investigate the stability of the systems (11)-(12), we represent the system in discrete form as

$$\boldsymbol{Y}\widehat{\boldsymbol{g}} = \mathfrak{b}, \tag{28}$$

the matrix $\boldsymbol{Y}_{N \times N}$ is sparse matrix obtained using localized RBF method. For the system (28) the constant of stability is defined as

$$\mathscr{C} = \sup_{\widehat{g} \ne 0} \frac{\|\widehat{\boldsymbol{g}}\|}{\|\boldsymbol{Y}\widehat{\boldsymbol{g}}\|}, \tag{29}$$

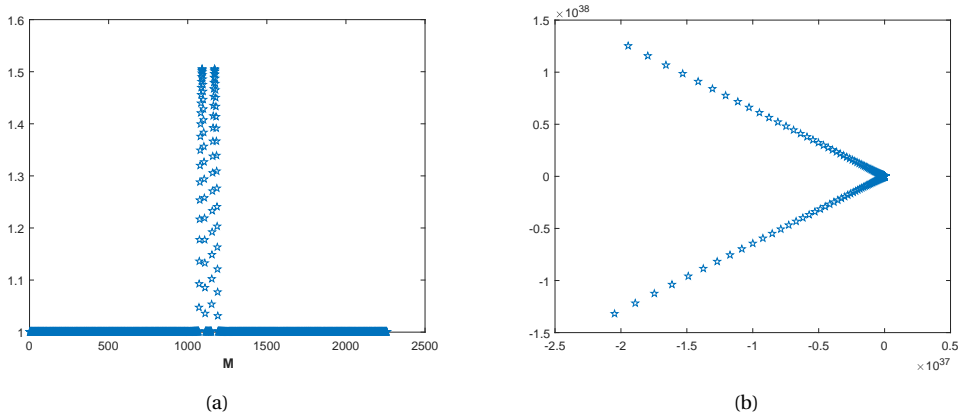(a)   (b)

Figure 1. In 1(a) corresponding to circular domain the constant $\mathscr{C}$ of stability is shown for the matrix $\boldsymbol{Y}$. In 1(b) the hyperbolic path is shown.

for any discrete norm $\|.\|$ defined on R^N the constant $\mathscr{C}$ is finite. From (29) we may write

$$\|\boldsymbol{Y}\|^{-1} \leq \frac{\|\widehat{\boldsymbol{g}}\|}{\|\boldsymbol{Y}\widehat{\boldsymbol{g}}\|} \leq \mathscr{C}, \tag{30}$$

Similarly for the pseudoinverse $\boldsymbol{Y}^\dagger$ of $\boldsymbol{Y}$, we can write

$$\left\|\boldsymbol{Y}^\dagger\right\| = \sup_{\boldsymbol{X}\neq 0} \frac{\left\|\boldsymbol{Y}^\dagger \boldsymbol{X}\right\|}{\|\boldsymbol{X}\|}. \tag{31}$$

Thus we have

$$\left\|\boldsymbol{Y}^\dagger\right\| \geq \sup_{\boldsymbol{X}=\boldsymbol{Y}\widehat{\boldsymbol{g}}\neq 0} \frac{\left\|\boldsymbol{Y}^\dagger \boldsymbol{Y}\widehat{\boldsymbol{g}}\right\|}{\|\boldsymbol{Y}\widehat{\boldsymbol{g}}\|} = \sup_{\widehat{\boldsymbol{g}}\neq 0} \frac{\|\widehat{\boldsymbol{g}}\|}{\|\boldsymbol{Y}\widehat{\boldsymbol{g}}\|} = \mathscr{C}. \tag{32}$$

We can see that Equations (30) and (32) confirms the bounds for the stability constant $\mathscr{C}$. Calculating the pseudoinverse for approximating the system (28) numerically be quite expansive computationally, but it confirms the stability. The MATLAB's function condest can be used to estimate $\|\boldsymbol{Y}^{-1}\|_\infty$ in case of square systems, thus we have

$$\mathscr{C} = \frac{condest\left(\boldsymbol{Y}'\right)}{\|\boldsymbol{Y}\|_\infty} \tag{33}$$

This work well with less number of computations for our sparse differentiation matrix $\boldsymbol{Y}$. Figure 1(a) shows the bounds for the constant C of our system (11)-(12) for the given problem corresponding to circular domain. Selecting $N = 500$, $M = 90$, $n = 15$, and $\alpha = 1.75$ at $t = 1$, we have $1.0003 \leq \mathscr{C} \leq 1.5053$. It is observed that the upper and lower bounds for the stability constant are very small numbers, which guarantees that the proposed localized RBF scheme is stable.

6. Numerical Experiments

In this section we implement our proposed Laplace transform based local RBF method for approximating solution of time fractional diffusion equation with CF derivative in square, circular and L-shape domains. In all our experiments we have utilized the Multiquadrics(MQ) kernels. The uncertainty principle [23] is utilized for optimal shape parameter. The accuracy is measured using the L_∞ and RMS errors which are given as

$$L_\infty = \left\| g(\mathbf{x}, t) - g_k(\mathbf{x}, t) \right\|_\infty = \max_{1 \le j \le N} \left(\left| g(\mathbf{x}, t) - g_k(\mathbf{x}, t) \right| \right),$$

and

$$RMS = \sqrt{\frac{\sum_j^N \left(g(\mathbf{x}_j, t) - g_k(\mathbf{x}_j, t) \right)^2}{N}},$$

where $g(\mathbf{x}, t)$, and $g_k(\mathbf{x}, t)$ are the exact and approximate solutions respectively.

To check the efficiency of the method we select the following two dimensional time fractional diffusion equation with CF derivative

$$\begin{matrix} CF \\ 0 \end{matrix} D_t^{\alpha+1} g(x, y, t) = \nabla g(x, y, t) + f(x, y, t), \tag{34}$$

where the forcing term $f(x, y, t)$ can be selected according to the exact solution. The problem is solved with zero initial conditions and the Dirichlet boundary conditions are generated from the exact solution given by

$$g(x, y, t) = t^{2+\alpha} \sin(\pi x) \sin(\pi y). \tag{35}$$

and the Robin boundary conditions

$$g(x, y, t) + \nabla g(x, y, t) \cdot \vec{n} = q(x, y, t), \ x, y \in \partial\Omega, \ t \in [0, 1]. \tag{36}$$

6.1. *Square Domain*

In the first test the square domain $[0, 1]^2$ is selected to approximate solution of the given problem using the proposed method. In this experiment the problem (34) is solved with Dirichlet boundary conditions extracted from the exact solution of the problem. The MATLAB's command $\xi = -M : k : M$ is used to generate the quadrature points along the path of integration Γ. The parameters used in our computations are $r = 0.1387, \delta = 0.1541, \theta = 0.1, \tau = \frac{t_0}{T}, \omega = 2, t \in [t_0, T]$ = [0.5, 5]. In our computations we used the Multiquadrics (MQ) kernel. In the Table 1 the results are obtained for various centers $n \in \Omega_i$ and $N \in \Omega$ with various quadrature points and α. The error estimates, L_∞ errors, the condition number κ, and the shape parameter ε are shown in Table 1. In Figure 1(a), the approximate and in Figure 1(b) exact solutions are shown. The regular nodes distribution in square domain is shown Figure 2(a), and the absolute error is shown in Figure 2(b). The results confirms the accuracy and efficiency of the proposed method.

Table 1. The results are obtained for different values of α, and $x, y \in [0, 1]^2$, at $t = 1$.

| $\alpha = 1.50$	N	n	M	L_∞ error	RMS error	$error_{est}$	ε	κ	CPU(s)
	441	12	40	2.90×10^{-3}	1.40×10^{-4}	1.83×10^{-1}	0.7	$3.03 \times 10^{+12}$	11.383506
			60	2.90×10^{-3}	1.40×10^{-4}	2.12×10^{-2}	0.7	$3.03 \times 10^{+12}$	25.811449
			70	2.90×10^{-3}	1.40×10^{-4}	7.20×10^{-3}	0.7	$3.03 \times 10^{+12}$	35.178792
			90	2.90×10^{-3}	1.40×10^{-4}	8.18×10^{-4}	0.7	$3.03 \times 10^{+12}$	59.738142
$\alpha = 1.95$	400	12	50	1.70×10^{-3}	8.48×10^{-5}	6.25×10^{-2}	0.7	$2.01 \times 10^{+12}$	23.881470
			60	1.70×10^{-3}	8.48×10^{-5}	2.12×10^{-2}	0.7	$2.01 \times 10^{+12}$	21.488349
			70	1.70×10^{-3}	8.48×10^{-5}	7.20×10^{-3}	0.7	$2.01 \times 10^{+12}$	29.542691
			80	1.70×10^{-3}	8.51×10^{-5}	2.40×10^{-3}	0.7	$2.01 \times 10^{+12}$	39.081166
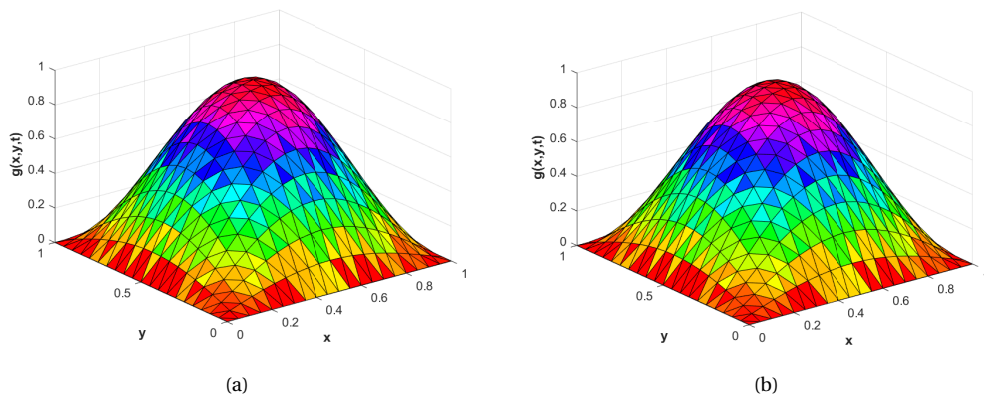
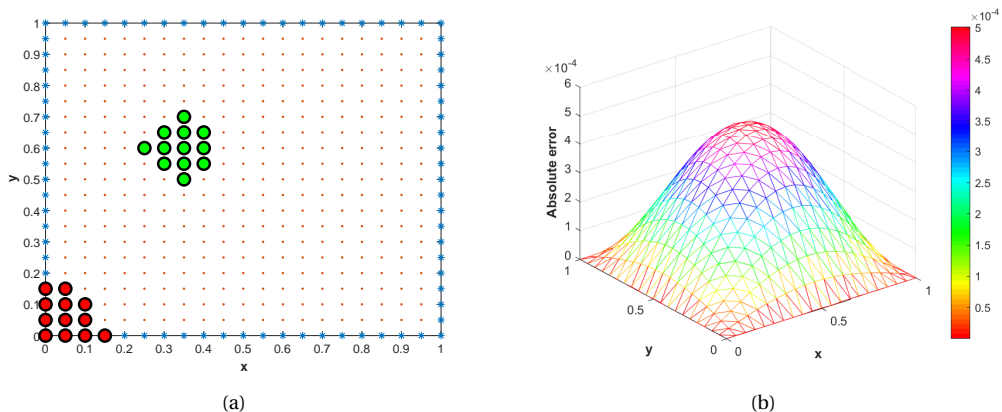**Figure 2.** In 2(a) the approximate solution is shown. In 2(b) the exact solution is shown.

Figure 3. In 3(a) the regular nodes distribution in square domain for $n = 12$, and $N = 441$ is depicted. In 3(b) the diagram of absolute error corresponding to problem 1 is shown for for $\alpha = 1.98, N = 441, n = 8$.

6.2. *Circular Domain*

Now we approximate the solution of the given problem in circular domain of radius $R = 1$ and centered at the origin. In this experiment we use the same set of parameters. Table 2 shows the results obtained using the proposed method in circular domain for $N = 500$, $n = 20$ different fractional orders α, and quadrature points. In this experiment also the problem (34) is solved using Dirichlet boundary conditions. From the results it can be observed that the proposed method produced accurate results. Figure 4(a), and Figure 4(b) present the approximate and exact solutions respectively. The computational domain with boundary stencil red and interior stencil green is shown in Figure 5(a), whereas Figure 5(b) depicts the absolute error.

7. L-Shape Domain

Here we apply the proposed method for approximating the solution of the time fractional 2D diffusion equation in L-shape domain. Here we use the same set of optimal parameters

Table 2. The RMS errors obtained for different values of α, at $t = 1$.

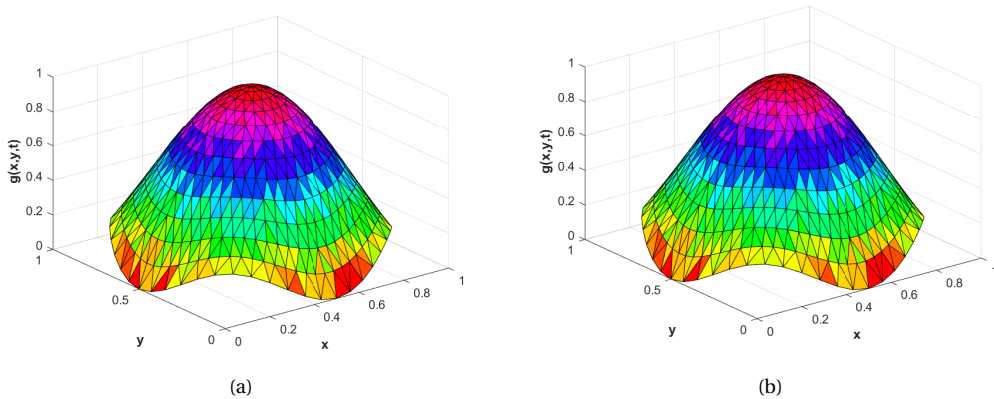| N	n	M	$\alpha = 1.25$	$\alpha = 1.5$	$\alpha = 1.65$	$\alpha = 1.85$	$\alpha = 1.95$
500	20	30	2.41×10^{-5}	2.37×10^{-5}	2.32×10^{-5}	2.23×10^{-5}	2.18×10^{-5}
		50	2.46×10^{-5}	2.37×10^{-5}	2.31×10^{-5}	2.21×10^{-5}	2.32×10^{-5}
		70	2.46×10^{-5}	2.37×10^{-5}	2.31×10^{-5}	2.21×10^{-5}	2.34×10^{-5}
		90	2.46×10^{-5}	2.37×10^{-5}	2.31×10^{-5}	2.22×10^{-5}	2.34×10^{-5}

(a)

(b)

Figure 4. In 4(a) the approximate solution for $N = 500$, $n = 15$, and $\alpha = 1.75$ is shown. In 4(b) the exact solution is shown.
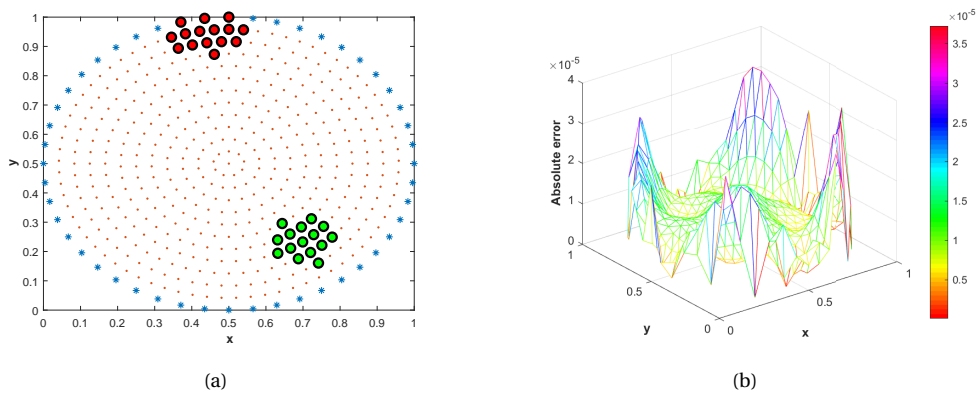

(a)

(b)

Figure 5. In 5(a) the regular nodes distribution in circular domain is shown. In 5(b) the absolute error for $\alpha = 1.90$, $N = 500$, $n = 25$ is shown.

which are used for square domain. The numerical results obtained using Dirichlet boundary conditions are shown in Table 3, where as the results obtained using Robin conditions defined in equation (36) are shown in Table (4). The results confirm the efficiency of the method in irregular domain. The graph of approximate and exact solution is shown in Figure 6(a), and the computational domain is depicted in Figure 6(b). The graph of RMS error using Dirichlet conditions is shown in Figure 7(a) and absolute error is shown in Figure 7(b). Figure 8 depicts the RMS error obtained using Robin conditions.

Table 3. The RMS errors obtained for different values of α, at $t = 1$.

N	n	M	$\alpha = 1.20$	$\alpha = 1.5$	$\alpha = 1.75$	$\alpha = 1.85$	$\alpha = 1.95$
833	19	30	3.88×10^{-5}	3.72×10^{-5}	3.61×10^{-5}	3.56×10^{-5}	3.52×10^{-5}
		50	3.80×10^{-5}	3.72×10^{-5}	3.62×10^{-5}	3.58×10^{-5}	3.62×10^{-5}
		70	3.80×10^{-5}	3.72×10^{-5}	3.62×10^{-5}	3.58×10^{-5}	3.81×10^{-5}
		90	3.80×10^{-5}	3.72×10^{-5}	3.62×10^{-5}	3.59×10^{-5}	3.42×10^{-5}

Table 4. The results are obtained for different quadrature nodes and $N = 736$, $n = 19$ at $t = 1$.

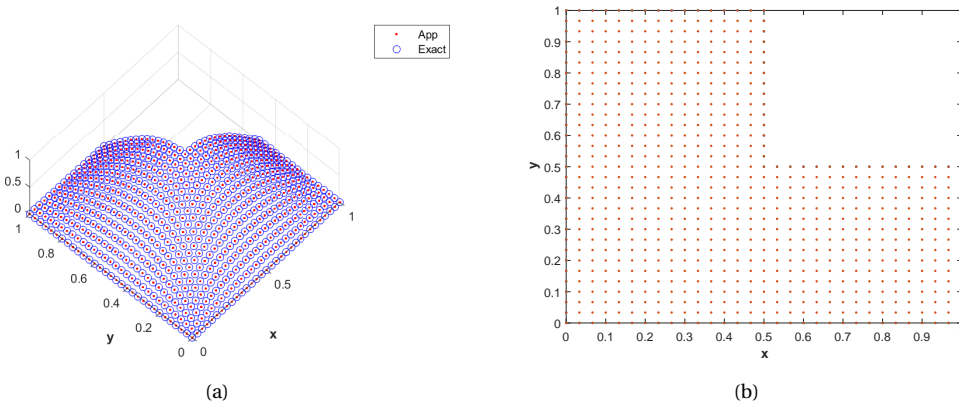| $\alpha = 1.90$	N	n	M	RMS error	$error_{est}$	ε	κ	CPU(s)
	736	19	40	4.80×10^{-3}	1.83×10^{-1}	2.0	$1.13 \times 10^{+12}$	42.315359
			60	4.80×10^{-3}	2.12×10^{-2}	2.0	$1.13 \times 10^{+12}$	93.625268
			70	4.80×10^{-3}	7.20×10^{-3}	2.0	$1.13 \times 10^{+12}$	129.241310
			90	4.80×10^{-3}	8.18×10^{-4}	2.0	$1.13 \times 10^{+12}$	214.265233

(a)   (b)

Figure 6. In 6(a) the approximate and exact solution for $\alpha = 1.80$ are shown. In 6(b) the computational domain is shown.

8. Conclusion

In the present work, we have successfully combined the LT with local RBFs for the approximation of the solution of of linear time fractional PDE with CF derivative. The Laplace transform have been used in combination with the local RBFs to eliminate the time variable and to avoid the stability restrictions which are commonly encountered in time stepping procedure. The bounds of stability and convergence of the method have been discussed. In our numerical experiments the Multiquadrics(MQ) kernel have been utilized. The experiments are carried out in square, circular, and L-shape domains. The results confirmed the efficiency and accuracy of the method. The benefit of this method is that it can solve such type of problems with less computation time with out any time instability. It was observed that the proposed method is capable of solving the linear fractional partial differential equations with CF derivative efficiently.
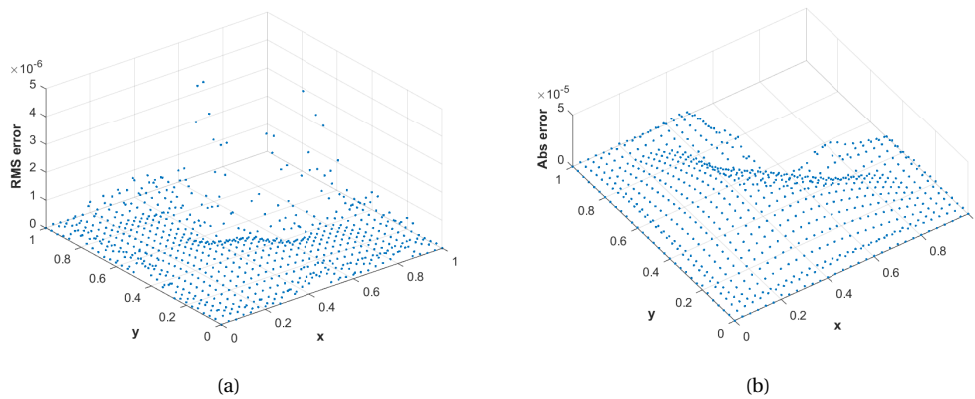
Figure 7. In 7(a) the RMS error for $\alpha = 1.95$, $N = 736$, $n = 19$ is shown. In 7(b) the absolute error for $\alpha = 1.80$, $N = 736$, $n = 20$ is shown.
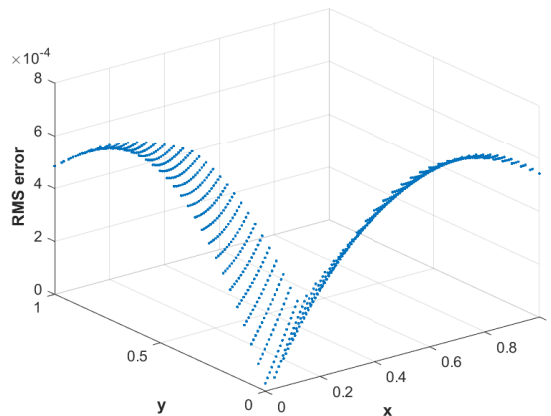

Figure 8. In Figure 8, the RMS error for $\alpha = 1.95$, $N = 736$, $n = 19$ is shown, when the problem is solved with Robin boundary conditions.

References

[1] O. J. J. Algahtani, "Comparing the Atangana–Baleanu and Caputo–Fabrizio derivative with fractional order: Allen Cahn model", *Chaos Solitons Fractals* **89** (2016), p. 552-559.

[2] S. Arshad, O. Defterli, D. Baleanu, "A second order accurate approximation for fractional derivatives with singular and non-singular kernel applied to a HIV model", *Appl. Math. Comput.* (2020), article ID 125061.

[3] A. Atangana, "On the new fractional derivative and application to nonlinear Fisher's reaction–diffusion equation", *Appl. Math. Comput.* **273** (2016), p. 948-956.

[4] A. Atangana, B. S. T. Alkahtani, "New model of groundwater flowing within a confine aquifer: application of Caputo-Fabrizio derivative", *Arab. J. Geosci.* **9** (2016), p. 8.

[5] A. Atangana, R. T. Alqahtani, "Numerical approximation of the space-time Caputo–Fabrizio fractional derivative and application to groundwater pollution equation", *Adv. Difference Equ.* (2016), article ID 156.

[6] M. Caputo, M. Fabrizio, "A new definition of fractional derivative without singular kernel", *Progr. Fract. Differ. Appl* **1** (2015), no. 2, p. 73-85.

[7] C. Cattani, H. M. Srivastava, X. J. Yang, *Fractional dynamics*, De Gruyter, 2015.

[8] E. F. Doungmo Goufo, "Application of the Caputo–Fabrizio fractional derivative without singular kernel to Korteweg–de Vries–Bergers equation", *Math. Model. Anal.* **21** (2016), no. 2, p. 188-198.

[9] E. F. Doungmo Goufo, M. K. Pene, J. N. Mwambakana, "Duplication in a model of rock fracture with fractional derivative without singular kernel", *Open Math.* **13** (2015), no. 1, p. 839-846.

[10] P. A. Feulefack, J. D. Djida, A. Atangana, "A new model of groundwater flow within an unconfined aquifer: Application of Caputo–Fabrizio fractional derivative", *Discrete Contin. Dyn. Syst.* **24** (2019), no. 7, p. 3227-3247.

[11] J. F. Gómez-Aguilar, H. Yépez-Martínez, C. Calderón-Ramón, I. Cruz-Orduña, R. F. Escobar-Jiménez, V. H. Olivares-Peregrino, "Modeling of a mass-spring-damper system by fractional derivatives with and without a singular kernel", *Entropy* **17** (2015), no. 9, p. 6289-6303.

[12] I. Jaradat, M. Alquran, S. Momani, D. Baleanu, "Numerical schemes for studying biomathematics model inherited with memory-time and delay-time", Article in press to appear in *Alexandria Engineering Journal*, https://www.sciencedirect.com/science/article/pii/S1110016820301472, 2020.

[13] Kamran, M. Uddin, A. Ali, "On the approximation of time-fractional telegraph equations using localized kernel-based method", *Adv. Differ. Equ.* (2018), article ID 305.

[14] A. A. Kilbas, H. M. Srivastava, J. J. Trujillo, *Theory and applications of fractional differential equations*, North-Holland Mathematics Studies, vol. 204, Elsevier, 2006.

[15] W. McLean, V. Thomée, "Numerical solution via Laplace transforms of a fractional order evolution equation", *J. Integral Equations Appl.* **22** (2010), no. 1, p. 57-94.

[16] I. A. Mirza, D. Vieru, "Fundamental solutions to advection–diffusion equation with time-fractional Caputo–Fabrizio derivative", *Comput. Math. Appl.* **73** (2017), no. 1, p. 1-10.

[17] V. F. Morales-Delgado, J. F. Gómez-Aguilar, H. Yépez-Martínez, D. Baleanu, R. F. Escobar-Jiménez, V. H. Olivares-Peregrino, "Laplace homotopy analysis method for solving linear partial differential equations using a fractional derivative with and without kernel singular", *Adv. Difference Equ.* **2016** (2016), no. 1, article ID 164.

[18] K. B. Oldham, J. Spanier, *The fractional calculus theory and applications of differentiation and integration to arbitrary order*, Mathematics in Science and Engineering, vol. 111, Academic Press Inc., 1974.

[19] K. M. Owolabi, A. Atangana, "Analysis and application of new fractional Adams–Bashforth scheme with Caputo–Fabrizio derivative", *Chaos Solitons Fractals* **105** (2017), p. 111-119.

[20] ———, "Numerical approximation of nonlinear fractional parabolic differential equations with Caputo–Fabrizio derivative in Riemann–Liouville sense", *Chaos Solitons Fractals* **99** (2017), p. 171-179.

[21] I. Podlubny, *Fractional differential equations. An introduction to fractional derivatives, fractional differential equations, to methods of their solution and some of their applications*, Mathematics in Science and Engineering, vol. 198, Academic Press, 1999.

[22] S. G. Samko, A. A. Kilbas, O. I. Marichev, *Fractional integrals and derivatives. Theory and applications*, Gordon and Breach Science Publishers, 1993.

[23] R. Schaback, "Error estimates and condition numbers for radial basis function interpolation", *Adv. Comput. Math.* **3** (1995), no. 3, p. 251-264.

[24] M. Uddin, Kamran, A. Ali, "A localized transform-based meshless method for solving time fractional wave-diffusion equation", *Eng. Anal. Bound. Elem.* **92** (2018), p. 108-113.

[25] H.-W. Zhou, S. Yang, S. Q. Zhang, "Modeling non-Darcian flow and solute transport in porous media with the Caputo–Fabrizio derivative", *Appl. Math. Modelling* **68** (2019), p. 603-615.